CrystEngComm

Accepted Manuscript

ROYAL SOCIETY OF CHEMISTRY

www.rsc.org/crystengcomm

CrystEngComm

Dynamic Article Links ►

Cite this: DOI: 10.1039/c4ce00000x

www.rsc.org/CrystEngComm

ARTICLE

Syntheses, Structures, and Magenetic Properties of Six Coordination Polymers Based on 4,5-Di(4'-carboxylphenyl)phthalic Acid and Different Bis(imidazole) Bridging Linkers

Liming Fan,[a] Yan Gao,[b] Guangzeng Liu,[b] Weiliu Fan,[a] Weikuo Song,[b] Liming Sun,[a] Xian Zhao,*[a] Xiutang Zhang*[a,b]

Received (in XXX, XXX) Xth XXXXXXXXX 2014, Accepted Xth XXXXXXXXX 2014
DOI: 10.1039/c4ce00000x

ABSTRACT: Six 4,5-di(4'-carboxylphenyl)phthalic acid (H_4DCP) based coordination polymers (CPs), namely, $\{[Ni(1,4\text{-bib})(HDCP)_2(H_2O)_2]_{0.5}[Ni(1,4\text{-bib})(H_2O)_4]\cdot 2H_2O\}_n$ (**1**), $[Ni(H_2DCP)(1,4\text{-bidb})_2(H_2O)]_n$ (**2**), $[Co_2(DCP)(1,3\text{-bib})]_n$ (**3**), $\{[Co_2(DCP)(1,4\text{-bidb})_2]\cdot 2H_2O\}_n$ (**4**), $[Co(H_2DCP)(4,4'\text{-bibp})]_n$ (**5**), and $[Co_2(DCP)(4,4'\text{-bibp})_2]_n$ (**6**), were synthesized under hydrothermal conditions in the presence of bis(imidazole) bridging linkers (1,3-bib = 1,3-bis(imidazol-1-yl)benzene, 1,4-bib = 1,4-bis(imidazol-1-yl)benzene, 1,4-bidb = 1,4-bis(imidazol-1-yl)-2,5-dimethyl benzene, 4,4'-bibp = 4,4'-bis(imidazol-1-yl)biphenyl). Their structures have been determined by single-crystal X-ray diffraction analyses and further characterized by elemental analyses, IR spectra, powder X-ray diffraction (PXRD), and thermogravimetric (TG) analyses. Single crystal X-ray diffraction analyses reveal that complex **1** is a cocrystal which consists of two independent chains. Complex **2** exhibits a traditional 2-fold 6^6-**dia** parallel entangled networks. Complex **3** dispalys a novel 3D binodal (5,7)-connected net based on binuclear $\{Co_2\}$ units with the Schläfli symbol of $(3.4^4.5^4.6)(3^2.4^8.5^8.6^3)$. Complex **4** shows a 2-fold binodal (4,4)-connected **bbf** net with the point symbol of $(6^4.8^6)(6^6)_2$. Complex **5** affords a 2D $(4^4.6^2)$-**sql** net constructed from $\{Co_2\}$ dinuclear units. Complex **6** dispalys a novel (3,8)-connected architecture with the Schläfli point symbol of $(4^2.5)_2(4^4.5^{10}.6^8.7^4.8^2)$ based on $\{Co_4(COO)_6\}$ SBUs. Magnetic studies indicate complexes **3** and **6** exhibit weak ferromagnetic and antiferromagnetic properties, respectively.

Introduction

Metal-organic coordination polymers (CPs), as an emerging class of inorgnic-organic hybrid materials, have attracted upsurging research interest not only because of their diverse structures and intersting topologies but also owing to their tremendous potential applications in gas storage and seperation, magnetism, luminescence, nonlinear optics, drug delivery, and heterogeneous catalysis.[1-4]

Generally speaking, such materials are constructed from the inorganic nodes (sigle metal ions, polynuclear metal cluster, SBUs) and organic linkers (polycarboxylate, N-donors, phosphonate, and so on) through non-covalent interactions.[5,6] And the structural diversities of designed CPs are mainly affected by two factors: the nature of organic ligands (internal factor, for example, the length, rigidly, coordination modes, functional groups, substituents of organic ligands) and the reaction conditions (external factor, such as, reaction temperature, templating agents, metal-ligand ratio, pH value, counteranion).[7-10] Among them, the synthesis controlled by ancillary ligands seemed more interetingly and operational, due to that different coligands hold different preferences when coordinating with metal centres.[11] When interacting with inorganic nodes, the coligands tend to adjust themselves to satisfy the needs of lowest system energy by twisting, rorating, and folding.[12] This strategy has been proved to be an efficient role for the assembly of structurally controllable CPs and inspires us to construct novel coordination materials.[13]

Here, by employing 4,5-di(4'-carboxylphenyl)phthalic acid (H_4DCP) and four different bis(imidazole) ancillary ligands (1,3-bib, 1,4-bib, 1,4-bidb, and 4,4'-bibp) (Scheme 1), six coordination polymers were obtained, namely, $\{[Ni_{0.5}(HDCP)(1,4\text{-bib})_{0.5}(H_2O)][Ni(1,4\text{-bib})(H_2O)_4]\cdot 2H_2O\}_n$ (**1**), $[Ni(H_2DCP)(1,4\text{-bidb})_2(H_2O)]_n$ (**2**), $[Co_2(DCP)(1,3\text{-bib})]_n$ (**3**), $\{[Co_2(DCP)(1,4\text{-bidb})_2]\cdot 2H_2O\}_n$ (**4**), $[Co(H_2DCP)(4,4'\text{-bibp})]_n$ (**5**), and $[Co_2(DCP)(4,4'\text{-bibp})_2]_n$ (**6**), which exhibit a systematic variation of architectures from 1D chains based cocrystal, 2D networks, to 3D frameworks. These results reveal that not only the nature of the bridging bis(imidazole) linkers (length, functional groups or substituent position) but also the reaction conditions (pH, metal ion) have great effect on the H_4DCP coordination modes and the final packing structures.

[a] *State Key Laboratory of Crystal Materials, Shandong University , Jinan 250100, China.*
E-mail: zhaoxian@icm.sdu.edu.cn.
[b] *Advanced Material Institute of Research, College of Chemistry and Chemical Engineering, Qilu Normal University, Jinan, 250013, China.*
E-mail: xiutangzhang@163.com.
†Electronic Supplementary Information (ESI) available: Additional Figures, IR spectrum, Powder XRD patterns and X-ray crystallographic data, CCDC 995908-995913 for **1-6**. See DOI: 10.1039/c4ce00000x.

Scheme 1. Structural characteristics of H_4DCP and structure related

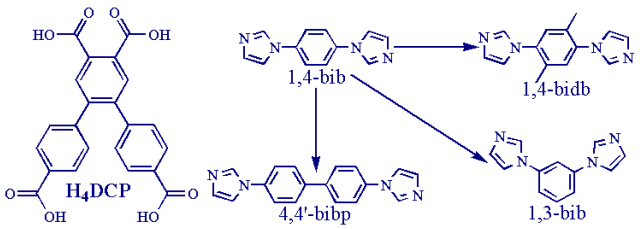

bis(imidazole) ancillary ligands.

Experimental Section

Materials and Physical Measurements. The chemicals of 4,5-di(4'-carboxylphenyl)phthalic acid, 1,3-bis(imidazol-1-yl)benzene, 1,4-bis(imidazol-1-yl)benzene, 1,4-bis(imidazol-1-yl)-2,5-dimethyl benzene, 4,4'-bis(imidazol-1-yl)biphenyl, 1,3-bis(imidazol-1-ylmethyl)benzene were purchased from Jinan Henghua Sci. & Tec. Co. Ltd. without further purification. IR spectra were measured on a Nicolet 740 FTIR Spectrometer at the range of 600-4000 cm^{-1}. Elemental analyses were carried out on a CE instruments EA 1110 elemental analyzer. TGA was measured from 25 to 800 °C on a SDT Q600 instrument at a heating rate 5 °C/min under the N_2 atmosphere (100 mL/min). X-ray powder diffractions were measured on a Panalytical X-Pert pro diffractometer with Cu-Kα radiation. The variable-temperature magnetic susceptibility measurements was performed on the Quantum Design SQUID MPMS XL-7 instruments in the temperature range of 2-300 K under a field of 1000 Oe.

General Synthesis Procedure for Complexes 1–6. The syntheses of **1**–**6** were performed in 25 mL Teflon-lined stainless steel autoclaves under autogenous pressure by utilizing the hydrothermal method. The one-pot mixture was heated to 170 °C for 72 h, and then cooled to room temperature at a descent rate of 10 °C/h. Finally, the crystals suitable for the single-crystal X-ray diffraction analysis were obtained.

Synthesis of $\{[Ni(1,4\text{-bib})(HDCP)_2(H_2O)_2]_{0.5}[Ni(1,4\text{-bib})(H_2O)_4]\cdot 2H_2O\}_n$ (1). A mixture of H_4DCP (0.10 mmol, 0.041g), 1,4-bib (0.20 mmol, 0.042 g), $NiSO_4\cdot 6H_2O$ (0.20 mmol, 0.053 g), NaOH (0.20 mmol, 0.008 g), and 12 mL H_2O was placed in a Teflon-lined stainless steel vessel, heated to 170 °C for 3 days, followed by slow cooling (a descent rate of 10 °C/h) to room temperature. Green block crystals of **1** were obtained. Yield of 51% (based on Ni). Anal. (%) calcd. for $C_{80}H_{80}N_{12}Ni_3O_{30}$: C, 51.50; H, 4.32; N, 9.01. Found: C, 50.79; H, 4.23; N, 8.89. IR (KBr pellet, cm^{-1}): 3357 (s), 3148 (s), 1702 (m), 1530 (vs), 1368 (m), 1238 (m), 833 (m),717 (w).

Synthesis of $[Ni(H_2DCP)(1,4\text{-bidb})_2(H_2O)]_n$ (2). A mixture of H_4DCP (0.10 mmol, 0.041g), 1,4-bidb (0.20 mmol, 0.045 g), $NiSO_4\cdot 6H_2O$ (0.20 mmol, 0.053 g), NaOH (0.20 mmol, 0.008 g), and 12 mL H_2O was placed in a Teflon-lined stainless steel vessel, heated to 170 °C for 3 days, followed by slow cooling (a descent rate of 10 °C/h) to room temperature. Green block crystals of **2** were obtained. Yield of 47% (based on Ni). Anal. (%) calcd. for $C_{50}H_{20}N_8NiO_9$: C, 64.20; H, 2.16; N, 11.98. Found: C, 63.81; H, 2.23; N, 11.59. IR (KBr pellet, cm^{-1}): 3368 (m), 3125 (m), 1582 (s), 1516 (vs), 1398 (vs), 1233 (m), 859 (m), 716 (w).

Synthesis of $[Co_2(DCP)(1,3\text{-bib})]_n$ (3). A mixture of H_4DCP (0.10 mmol, 0.041g), 1,3-bib (0.20 mmol, 0.042 g), $CoCl_2\cdot 6H_2O$ (0.20 mmol, 0.048 g), NaOH (0.20 mmol, 0.008 g), and 12 mL H_2O was placed in a Teflon-lined stainless steel vessel, heated to 170 °C for 3 days, followed by slow cooling (a descent rate of 10 °C/h) to room temperature. Violet block crystals of **3** were obtained. Yield of 57% (based on Co). Anal. (%) calcd. for $C_{34}H_{20}Co_2N_4O_8$: C, 55.91; H, 2.76; N, 7.67. Found: C, 55.77; H, 2.69; N, 7.39. IR (KBr pellet, cm^{-1}): 3061 (w), 1602 (m), 1578 (vs), 1522 (s), 1395 (vs), 1262 (m), 782 (m), 724 (w).

Synthesis of $\{[Co_2(DCP)(1,4\text{-bidb})_2]\cdot 2H_2O\}_n$ (4). A mixture of H_4DCP (0.10 mmol, 0.041g), 1,4-bidb (0.20 mmol, 0.045 g), $CoCl_2\cdot 6H_2O$ (0.20 mmol, 0.048 g), NaOH (0.20 mmol, 0.008 g), and 12 mL H_2O was placed in a Teflon-lined stainless steel vessel, heated to 170 °C for 3 days, followed by slow cooling (a descent rate of 10 °C/h) to room temperature. Purple block crystals of **4** were obtained. Yield of 63% (based on Co). Anal. (%) calcd. for $C_{34}H_{20}Co_2N_4O_8$: C, 55.91; H, 2.76; N, 7.67. Found: C, 60.01; H, 2.79; N, 7.43. IR (KBr pellet, cm^{-1}): 3380 (m), 3125 (m), 1604 (s), 1559 (m), 1520 (s), 1368 (s), 1068 (s), 853 (m), 785 (w).

Synthesis of $[Co(H_2DCP)(4,4'\text{-bibp})]_n$ (5). A mixture of H_4DCP (0.15 mmol, 0.062g), 4,4'-bibp (0.20 mmol, 0.057 g), $CoCl_2\cdot 6H_2O$ (0.30 mmol, 0.059 g), NaOH (0.20 mmol, 0.008 g), and 12 mL H_2O was placed in a Teflon-lined stainless steel vessel, heated to 170 °C for 3 days, followed by slow cooling (a descent rate of 10 °C/h) to room temperature. Pink block crystals of **5** were obtained. Yield of 53% (based on Co). Anal. (%) calcd. for $C_{40}H_{26}CoN_4O_8$: C, 64.10; H, 3.50; N, 7.47. Found: C, 63.97; H, 3.69; N, 7.28. IR (KBr pellet, cm^{-1}): 3135 (m), 1587 (s), 1516 (s), 1351 (s), 1307 (s), 1243 (m), 1061 (m), 815 (m), 783 (m).

Synthesis of $[Co_2(DCP)(4,4'\text{-bibp})_2]_n$ (6). The same synthetic procedure as for **5** was used except that 0.2 mmol NaOH was replaced by 0.6 mmol NaOH, giving violet block crystals. Yield of 43% (based on Co). Anal. (%) calcd. for $C_{58}H_{38}Co_2N_8O_8$: C, 63.74; H, 3.50; N, 10.25. Found: C, 62.63; H, 3.74; N, 9.87. IR (KBr pellet, cm^{-1}): 3143 (m), 1668 (w), 1589 (m), 1549 (w), 1515 (s), 1401 (s), 1345 (s), 811 (m), 714 (m).

X-ray crystallography. Intensity data collection was carried out on a Siemens SMART diffractometer equipped with a CCD detector using Mo-*Kα* monochromatized radiation (λ = 0.71073 Å) at 293(2) or 296(2) K. The absorption correction was based on multiple and symmetry-equivalent reflections in the data set using the SADABS program based on the method of Blessing. The structures were solved by direct methods and refined by full-matrix least-squares using the SHELXTL package.[14] Crystallographic data for complexes **1**–**6** are given in Table 1. Selected bond lengths and angles for **1**–**6** are listed in Table S1. For complexes of **1**–**6**, further details on the crystal structure investigations may be obtained from the Cambridge Crystallographic Data Centre, CCDC, 12 Union Road, CAMBRIDGE CB2 1EZ, UK, [Telephone:+44-(0)1223-762-910, Fax: +44-(0)1223-336-033; Email: deposit@ccdc.cam.ac.uk, http://www.ccdc.cam.ac.uk/deposit], on quoting the depository number CCDC-995908 for **1**, 995909 for **2**, 995910 for **3**, 995911 for **4**, 995912 for **5**, and 995913 for **6**. Topological analysis of the coordination networks of all the compounds was performed with the program package TOPOS.[15]

Result and discussion

Synthesis and Characterization. Complexes **1-6** were constructed from H_4DCP and the related Co^{II}/Ni^{II} salts in the presence of four bis(imidazole) ancillary ligands (1,3-bib, 1,4-bib, 1,4-bidb, and 4,4'-bibp) under hydrothermal conditions. Complexes **1-6** are stable in the solid state upon extended exposure to air. They have poor solubility in water and common organic solvents, but can be slightly soluble in very high polarity solvents, such as DMF, DMSO.

Powder X-ray diffraction (PXRD) has been used to check the phase purity of the bulk samples in the solid state. For complexes **1**−**6**, the measured PXRD patterns closely match the simulated patterns generated from the results of single crystal diffraction data, indicative of pure products (Fig. S1, see Supporting Information). The absorption bands in the range of 3300-3500 cm^{-1} for **1-6** can be attributed to the characteristic peaks of water O-H vibrations. The vibrations at ca. 1500 and 1610 cm^{-1} correspond to the asymmetric and symmetric stretching vibrations of the carboxyl groups, respectively (Fig. S2).

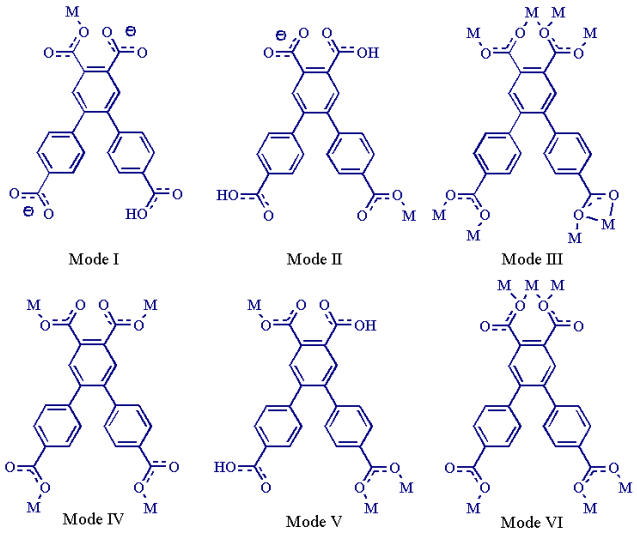

Scheme 2. The coordination modes of H_4DCP in complexes **1-6**.

Table 1 Crystal data for **1 – 6**.

Compound	**1**	**2**	**3**	**4**	**5**	**6**
Empirical formula	$C_{80}H_{80}N_{12}Ni_3O_{30}$	$C_{50}H_{20}N_8NiO_9$	$C_{34}H_{20}Co_2N_4O_8$	$C_{50}H_{42}Co_2N_8O_{10}$	$C_{40}H_{26}CoN_4O_8$	$C_{58}H_{38}Co_2N_8O_8$
Formula weight	1865.69	957.63	730.40	1032.78	749.58	1092.82
Crystal system	Triclinic	Monoclinic	Monoclinic	Monoclinic	Triclinic	Monoclinic
Space group	*P-1*	*P2₁/n*	*C2/c*	*C2/c*	*P-1*	*C2/c*
a (Å)	7.7686(11)	14.649(2)	19.7798(6)	15.59(3)	10.3636(9)	33.6935(18)
b (Å)	13.6512(7)	13.470(2)	12.5466(11)	16.36(3)	12.2034(11)	11.1225(6)
c (Å)	19.8766(11)	24.399(4)	25.8545(6)	21.03(3)	14.0163(12)	27.5859(14)
α (°)	99.250(3)	90.00	90.00	90.00	89.208(2)	90.00
β (°)	94.563(3)	106.607(3)	110.619(3)	120.49(11)	73.7390(10)	114.0270(10)
γ (°)	97.512(3)	90.00	90.00	90.00	75.8750(10)	90.00
V(Å^3)	2051.7(3)	4613.9(13)	6005.3(6)	4622(14)	1647.5(2)	9442.2(9)
Z	1	4	8	4	2	8
D_{calcd} (Mg/m^3)	1.510	1.379	1.616	1.484	1.511	1.537
μ(mm^{-1})	0.774	0.487	1.167	0.788	0.586	0.773
θ range (°)	1.04–25.00	1.74–25.00	1.68–25.00	1.96–25.00	1.72–25.00	1.95–25.00
Reflections collected	10422	23121	12169	22842	8514	23757
Data/Parameters	7179/551	8128/625	5268/433	8025/636	5785/480	8306/685
F(000)	968	1992	2960	228	770	4480
T(K)	296(2)	296(2)	296(2)	293(2)	296(2)	293(2)
R_{int}	0.0319	0.0418	0.0486	0.1289	0.0257	0.0522
R_1 (wR_2) [$I > 2\sigma(I)$]	0.0508 (0.1370)	0.0409 (0.0976)	0.0433(0.1093)	0.0661 (0.1310)	0.0439 (0.1110)	0.0441 (0.1063)
R_1 (wR_2) (all data)	0.0836 (0.1621)	0.0601 (0.1079)	0.0674 (0.1228)	0.1510 (0.1626)	0.0621 (0.1297)	0.0726 (0.1240)
Gof	0.998	1.000	0.998	0.999	1.003	1.000

$R_1 = \Sigma||F_o|-|F_c||/\Sigma|F_o|$, $wR_2 = [\Sigma w(F_o^2-F_c^2)^2]/\Sigma w(F_o^2)^2]^{1/2}$

Structural Description of $\{[Ni(1,4\text{-bib})(HDCP)_2(H_2O)_2]_{0.5}[Ni(1,4\text{-bib})(H_2O)_4]\cdot 2H_2O\}_n$ (1). X-ray diffraction analysis revealed that complex **1** crystallized in the triclinic system, space group *P*-1, and was made up of two kinds of species: 1D $\{[Ni(1,4\text{-bib})(HDCP)_2(H_2O)_2]^{2-}\}_n$ chain and 1D $\{[Ni(1,4\text{-bib})(H_2O)_4]^{2+}\}_n$ chain. The asymmetric unit of **1** contains one and a half crystallographically independent Ni^{II} ions, one $HDCP^{3-}$ ligand, one and a half of 1,4-bib ligands, five coordinated water molecules, and two lattice water molecules (Fig. 1a). Ni1 is hexa-coordinated by two N atoms from two 1,4-bib ligands, four O atoms from two $HDCP^{3-}$ ligands, and two coordinated water molecules. Ni2 is coordinated by two N atoms from two another 1,4-bib ligands and four water O atoms, showing a distorted octahedral coordination geometry. The bond lengths of Ni–O and Ni–N are in the normal range of 2.050(2)–2.123(4) Å and 2.067(5)–2.080(5) Å, respectively.

In complex **1**, Ni^{II} ions are linked by 1,4-bib ligands to form 1D anionic chain of $\{[Ni(1,4\text{-bib})(HDCP)_2(H_2O)_2]^{2-}\}_n$ and 1D cationic chain of $\{[Ni(1,4\text{-bib})(H_2O)_4]^{2+}\}_n$. In the anionic chain, the geometry of Ni^{II} is saturated by four oxygen atoms from two carboxylate oxygen and two associated water molecules. Whereas, Ni^{II} in the cationic one is coordinated by four water molecules. The Ni···Ni distances in anionic chain is a little longer than the one in the cationic one, which maybe attributed to the stereospecific blockade from $HDCP^{3-}$. The ionized carboxyl groups in **1** act as hydrogen bond acceptor and the charge balancing, which play a critical role on maintaining the overall structure stability (Table 2). It is also noteworthy that the other hydrogen bonds as well as π···π interactions [Cg···Cg = 3.884(4) Å] between phenyl rings of 1,4-bib ligands from the two kinds of chains act as a solidification in constructing the 3D supramolecular (Fig. 1c). For the intuitive understanding, the final structure was simplified, shown in Fig. 1d.

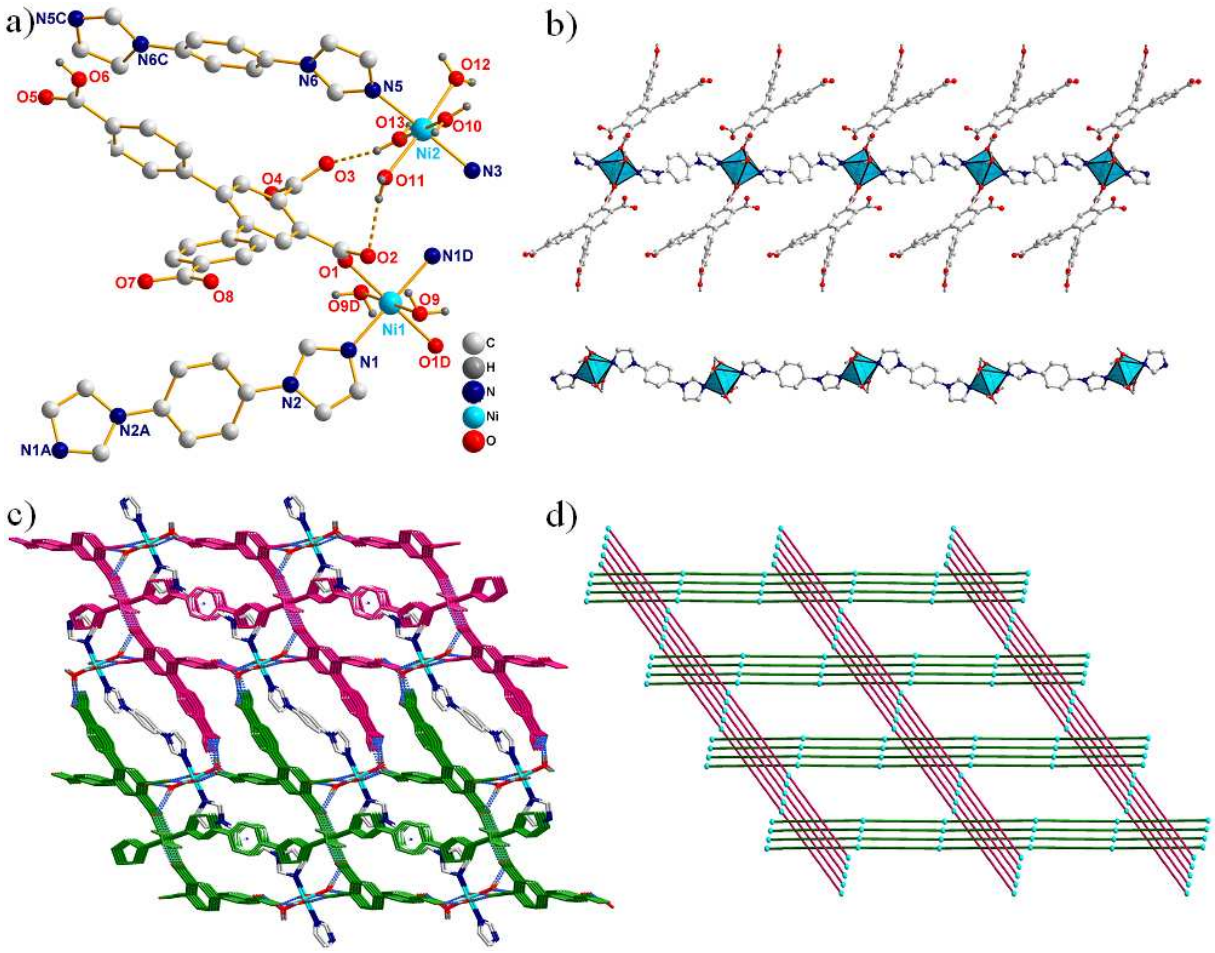

Figure 1. (a) Coordination environment of Ni^{II} ions in complex **1** (Symmetry codes: A: -*x*, 2-*y*, 1-*z*; C: -*x*, 1-*y*, -*z*; D: -*x*, 1-*y*, 1-*z*). (b) Two independent 1D chains in constructed complex **1**. (c) The hydrogen bonds and π···π interactions based 3D supramolecular. (d) The simplified structure of complex **1** (Red chains: $[Ni_{0.5}(HDCP)(1,4\text{-bib})_{0.5}(H_2O)]_n^{2n-}$ chains; Grass green chains: $[Ni(1,4\text{-bib})(H_2O)_4]_n^{2n+}$ chains).

Table 2 Hydrogen bonds data in complex **1**[a].

D–H···A	d(D···A)/Å	d(H···A)/Å	∠(D–H···A)/deg
O(11)-H(6w)-O(2)	2.800	1.992	168.79
O(13)-H(10w)-O(3)	2.729	1.956	156.86
O(9)-H(1w)-O(14)	2.777	1.996	158.82
O(14)-H(11w)-O(2)$^{\#1}$	2.789	2.021	155.68
O(10)-H(4w)-O(3)$^{\#2}$	2.717	1.899	174.02
O(11)-H(5w)-O(4)$^{\#2}$	2.621	1.820	164.72
O(15)-H(13w)-O(4)$^{\#2}$	3.011	2.267	146.90
O(14)-H(12w)-O(4)$^{\#3}$	2.871	2.109	154.31
O(12)-H(8w)-O(5)$^{\#4}$	2.846	2.070	157.78
O(10)-H(3w)-O(7)$^{\#5}$	2.860	2.085	156.92
O(13)-H(9w)-O(7)$^{\#6}$	2.739	1.924	172.11
O(12)-H(7w)-O(8)$^{\#6}$	2.695	1.900	162.87
O(6)-H(6)-O(7)$^{\#7}$	2.665	1.856	168.54

[a] Symmetry codes: #1: -*x*+1, -*y*+1, -*z*+1; #2: *x*+1, *y*, *z*; #3: -*x*, -*y*+1, -*z*+1; #4: -*x*, -*y*+1, -*z*; #5 *x*, *y*-1, *z*; #6: *x*−1, *y*-1, *z*; #7: -*x*+1, -*y*+2, -*z*.

Structural Description of $[Ni(H_2DCP)(1,4\text{-bidb})_2(H_2O)]_n$ (2). The similar synthetic method to compound **1** was employed, except for two methyl groups on 1,4-bib ligand. Out of expectation, the three-dimensional architecture was obtained. Complex **2** crystallizes in the monoclinic system, space group $P2_1/n$ and the asymmetric unit contains one crystallographically independent Ni^{II} ion, one H_2DCP^{2-} anion, two 1,4-bidb ligands, and one coordinated water molecule (Fig. 2a). Each Ni^{II} ion shows distorted $\{NiO_2N_4\}$ octahedral geometry, completed by four N atom from four 1,4-bidb ligands and two O atoms from one H_2DCP^{2-} anion and water molecule. The bond lengths of Ni-N are in the range of 2.077(2)-2.098(2) Å, and the Ni-O are 2.0684(17) and 2.1178(19) Å, respectively.

Similar to compound **1**, H_4DCP ligand in **2** is also partly deprotonated and owns mono-dentate coordination mode (Mode II, Scheme 2). Due to the steric effect of two methyl groups from 1,4-bidb ligand, the suitable torsion angles between neighbouring 1,4-bidb result in that Ni^{2+} ions are connected by 1,4-bidb to form a 3D porous $[Ni(1,4\text{-bidb})_2]_n$ framework (Fig. 2b), rather than 1D chain in complex **1**. The adjacent Ni···Ni distances in the 3D framework are 13.131 Å, 13.464 Å, and 13.476 Å, respectively. H_2DCP^{2-} ligands fulfilled the void channels and modified the 3D framework at the same times (Fig. 2c). Moreover, the two independent frameworks interact with each other *via* hydrogen bonds O(4)-H(4A)···O(2)$^{\#1}$=2.597 Å, O(9)-H(2w)···O(5)$^{\#2}$=2.710 Å, Symmetry codes: #1: *x*+1/2, -*y*+1/2, *z*+1/2; #2: *x*+1/2, -*y*+1/2, *z*-1/2.) to make the whole structure stable. From the viewpoint of topology, each Ni^{II} ion can be simplified to 4-connected nodes, and the final structure of complex **2** can be regarded as 2-fold 6^6-**dia** nets (Fig. 2d).

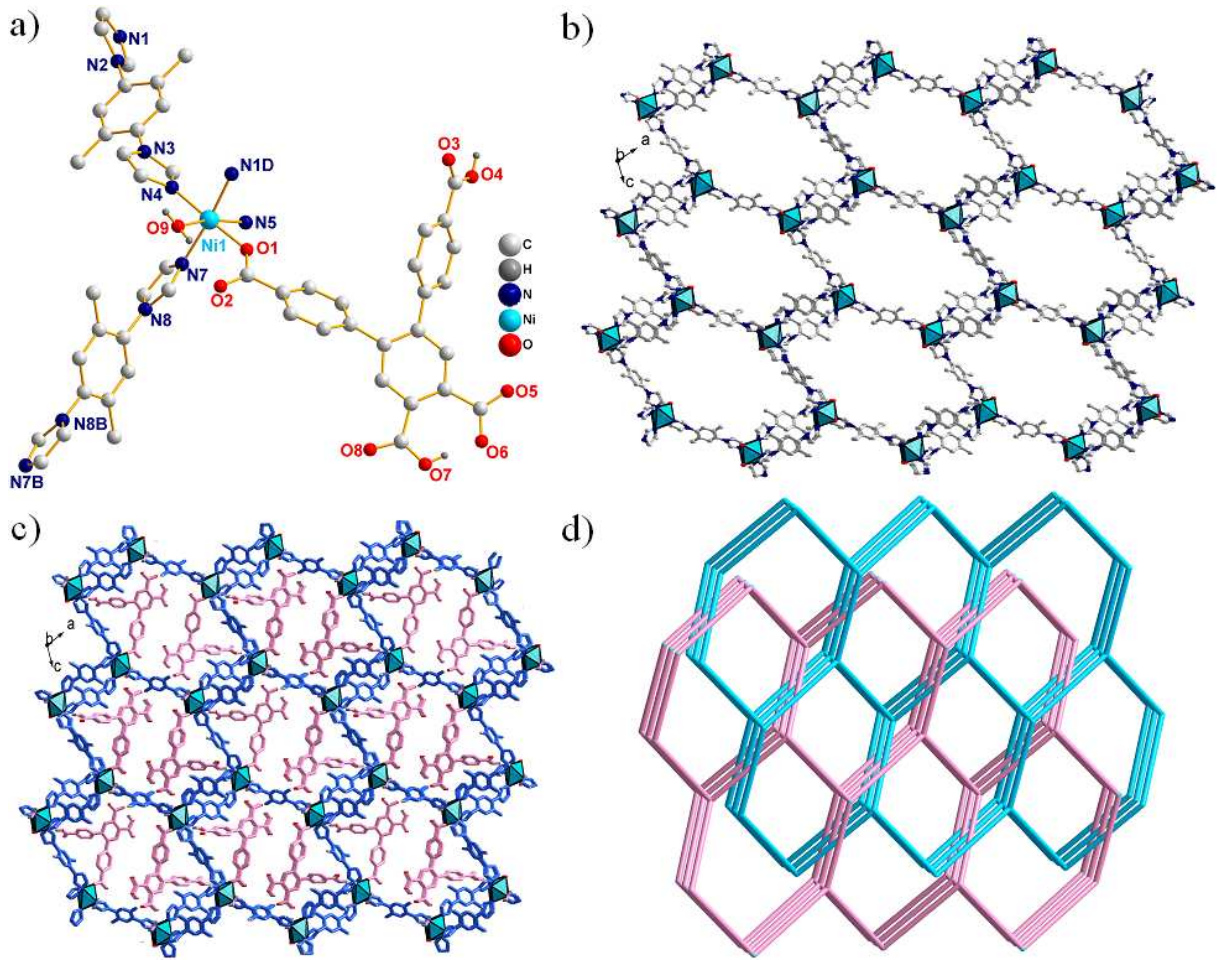

Figure 2. (a) Coordination environment of Ni^{II} ion in **2** (Symmetry codes: B: *–x*, *–y*, *–z*; D: 1.5*–x*, 0.5+*y*, 0.5*–z*.). (b) View of the 3D $[Ni(1,4\text{-bidb})_2]_n$ networks. (c) The 3D structure frameworks of **2**. (d) Schematic view of the 2-fold 4-connected 6^6-**dia** nets of **2**.

Structural Description of $[Co_2(DCP)(1,3\text{-bib})]_n$ (3). Structure analysis reveals that complex **3** crystallizes in the monoclinic system, space group *C2/c*. The asymmetric unit contains two Co^{II} ions, one DCP^{4-} ligand, and one 1,3-bib ligand (Fig. 3a). Both Co1 and Co2 ions display similar distorted octahedral geometries, which are completed by one N atom and five O atoms from four different DCP^{4-} ligands. The bond lengths of Co-O are in the range of 2.012(3)-2.338(3) Å, and the Co-N bond length are 2.067(3) and 2.138(3) Å, respectively.

As shown in Scheme 2, each DCP^{4-} ligand coordinated with eight Co^{II} ions by adopting $(\kappa^1\text{-}\kappa^1)\text{-}(\kappa^2\text{-}\kappa^1)\text{-}(\kappa^1\text{-}\kappa^2)\text{-}(\kappa^1\text{-}\kappa^1)\text{-}\mu_8$ coordination mode (Mode III), in which the four carboxyl groups show $(\kappa^1\text{-}\kappa^1)\text{-}\mu_2$, $(\kappa^1\text{-}\kappa^2)\text{-}\mu_2$, and $(\kappa^1\text{-}\kappa^2)\text{-}\mu_3$ coordination fashions, respectively. Besides, the dihedral angles between three phenyl rings in DCP^{4-} are 74.59(3), 54.56(0), and 70.77(7)°, respectively. The two neighbouring Co^{II} ions are connected by $(\kappa^1\text{-}\kappa^2)\text{-}\mu_3$ and $(\kappa^1\text{-}\kappa^2)\text{-}\mu_2$ carboxyl groups, affording a binuclear $\{Co_2\}$ unit by edge-sharing with the distance being 3.172 Å between Co1 and Co2. And the $\{Co_2\}$ units are further connected by the $(\kappa^1\text{-}\kappa^1)\text{-}\mu_2$ carboxyl groups, finally giving an unusual 1D $[Co_4(COO)_8]_n$ chain (Fig. S3). Then the 1D $[Co_4(COO)_8]_n$ chains are linked by another DCP^{4-} to yield 3D $[Co_2(BCP)]_n$ frameworks (Fig. 3b). Furthermore, the 1,3-bib ligands modified the $[Co_2(BCP)]_n$ frameworks along the $[Co_4(COO)_8]_n$ chain, giving the 3D frameworks (Fig. 3c). PLATON software revealed the void volume of **3** is 10.8 % of the crystal volume (647.8 out of the 6005.3 $Å^3$ unit cell volume).[16]

To illustrate the unique structure of **3**, the topological analysis approach is employed. From the topological point of view, the $\{Co_2\}$ cluster can be simplified to 7-connected nodes, and the DCP^{4-} ligands linked with five $\{Co_2\}$ clusters, was regarded as 5-connected nodes, giving rise to an novel binodal (5,7)-connected nets with the point symbol of $(3.4^4.5^4.6)(3^2.4^8.5^8.6^3)$ (Fig. 3d).

Structure descriptions of $\{[Co_2(DCP)(1,4\text{-bidb})_2]\cdot 2H_2O\}_n$ (4). When 1,4-bidb was introduced into the reaction system, complex **4** was obtained. X-ray single-crystal diffraction analysis reveals that complex **4** is a 3D porous framework. There are two Co^{II} ions, one DCP^{4-} ligand, two 1,4-bidb ligands, and two lattice water molecules in the asymmetric unit. As shown in Fig.4a, the environment around Co1 can be described as a distorted tetrahedron geometry, coordinated by two O atoms from two DCP^{4-} ligands and two N atoms from two 1,4-bidb ligands. Similarly, each Co2 is coordinated by two O atoms from two DCP^{4-} ligands, and two N atoms from two 1,4-bidb ligands, forming a slightly distorted tetrahedral geometry with the $\{CoN_2O_2\}$ coordination environment. The bond lengths of Co–O and Co–N are in the range of 1.914(4)–2.383(6) Å and 1.949(5)–1.998(5) Å, respectively.

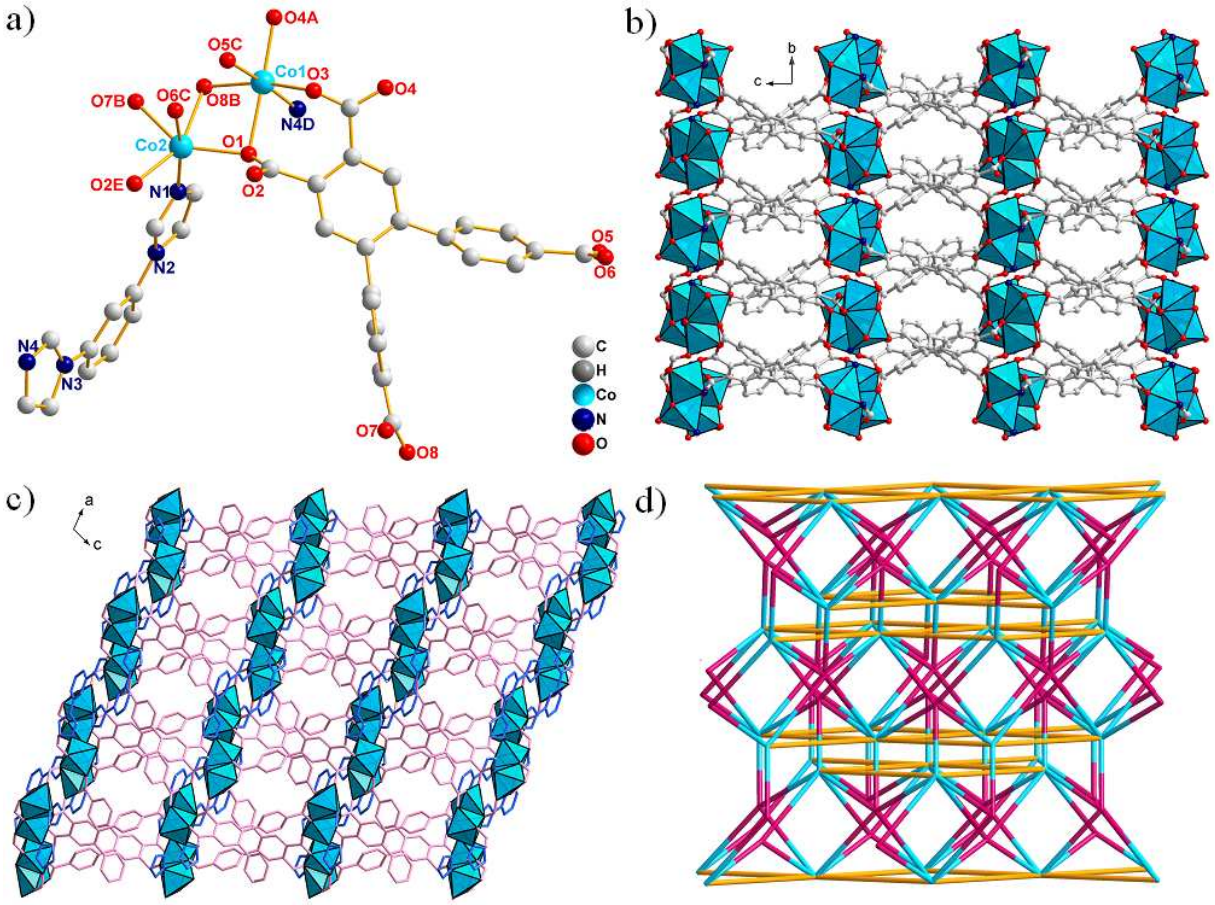

Figure 3. Coordination environment of Co^{II} ions in **3** (Symmetry codes: A: 1–*x*, 1–*y*, 2-*z*; B: 0.5+*x*, 1.5–*y*, 0.5+*z*; C: *x*, 1–*y*, 0.5+*z*; E: 0.5–*x*, 1.5–*y*, 2–*z*.). (b) View of the 3D $[Co_2(DCP)]_n$ networks based on 1D $[Co_4(COO)_8]_n$ chains. (c) The 3D structure frameworks of **3**. (d) Schematic view of the (5,7)-connected nets of **3** (green spheres: $\{Co_2\}$ SBUs; red spheres: DCP^{4-} ligands; yellow bonds: 1,3-bib ligands).

It is worth noting that the DCP^{4-} exhibits $(\kappa^1\text{-}\kappa^0)\text{-}(\kappa^0\text{-}\kappa^1)\text{-}(\kappa^0\text{-}\kappa^1)\text{-}(\kappa^1\text{-}\kappa^0)\text{-}\mu_4$ coordination mode (Mode V, Scheme 2) and connect four Co^{II} ions with four monodentate carboxyl groups, forming a 2D $[Co_2(DCP)]_n$ network with the opening area is 11.606(6) ×14.539(9) $Å^2$ (Fig. 4b). The Co···Co distances separated by DCP^{4-} ligands are 6.843(1), 9.683(0), 11.948(3), and 12.646(5) Å (Fig. S4). The dihedral angles between three phenyl rings in DCP^{4-} are 60.11(6)°/52.72(5)°/56.98(7)°, which indicated the DCP^{4-} ligand twisted to satisfy the preferences of Co^{II} ions. The 2D networks are further expanded by connected with the bridging 1,4-bidb ligand, finally given a porous 3D framework (Fig. 4c). It is noteworthy that the guest molecules occupied the channels and interact with the host framework *via* hydrogen bonds, which may be one important factor to stabilize the whole framework. Two adjacent frameworks interacted with each other, make the whole structure more stable. Besides, PLATON calculated the void volume of **4** is 5.0 % (230.7 out of the 4623.3 $Å^3$ unit cell volume).

The topology analysis shows that the overall framework of complex **4** can be rationalized to a 2-fold binodal (4,4)-connected **bbf** net with the point symbol of $(6^4.8^6)(6^6)_2$ by denoting DCP^{4-}, Co(1), and Co(2) all as 4-connected nodes, respectively (Fig. 4d).

Structure descriptions of $[Co(H_2DCP)(4,4'\text{-bibp})]_n$ (5). With the purpose of exploring new materials, the longer bis(imidazole) linker(4,4'-bibp) was employed in the reaction system. Structure analysis reveals that complex **5** crystallizes in the triclinic system, space group *P*-1. The asymmetric unit of **5** contains one Co^{II} ion, one partly deprotonated H_2DCP^{2-} ligand, and one 4,4'-bibp ligand, shown in Fig. 5a. The Co^{II} ion is surrounded by three H_2DCP^{2-} anions and two 4,4'-bibp ligands, leaving a distorted $\{CoN_2O_3\}$ coordination environment. The Co-N/O bond lengths are in the normal range.

The H_4DCP is partly deprotonated and connected two Co^{II} ions with $(\kappa^1\text{-}\kappa^0)\text{-}(\kappa^1\text{-}\kappa^1)\text{-}\mu_3$ coordination mode (Mode V, Scheme 2). The dihedral angles between three phenyl rings in H_2DCP^{4-} are 39.38(0), 75.39(5), and 67.72(2)°, respectively. Two Co^{II} ions were connected by the $(\kappa^1\text{-}\kappa^1)\text{-}\mu_2$ carboxyl group, forming a $\{Co_2\}$ SBUs, which can be view as the shared nodal. The distances separated by H_2DCP^{2-} and 4,4'-bibp between adjacent SBUs are 14.917 Å and 17.834 Å, respectively (Fig. 5b). The two 1D chains are further intersected with each other by sharing the SBUs, finally giving a 2D bilayer sheet with a 14.917×17.834 $Å^2$ quadrilateral opening (Fig. 5c). The supporting hydrogen bonds between two neighbouring sheets make the final packing structure more stable (O(5)-H(5A)···$O(4)^{\#1}$=2.617 Å, Symmetry codes: #1: *x*-1, *y*+1, *z*.).

From the viewpoint of structural topology, the whole structure of complex **5** can be defined as a 4-connected $(4^4.6^2)$-**sql** topology by denoting the $\{Co_2\}$ SBUs to four connected nodes and H_2DCP^{2-} and 4,4'-bibp ligands as linkers (Fig. 5d).

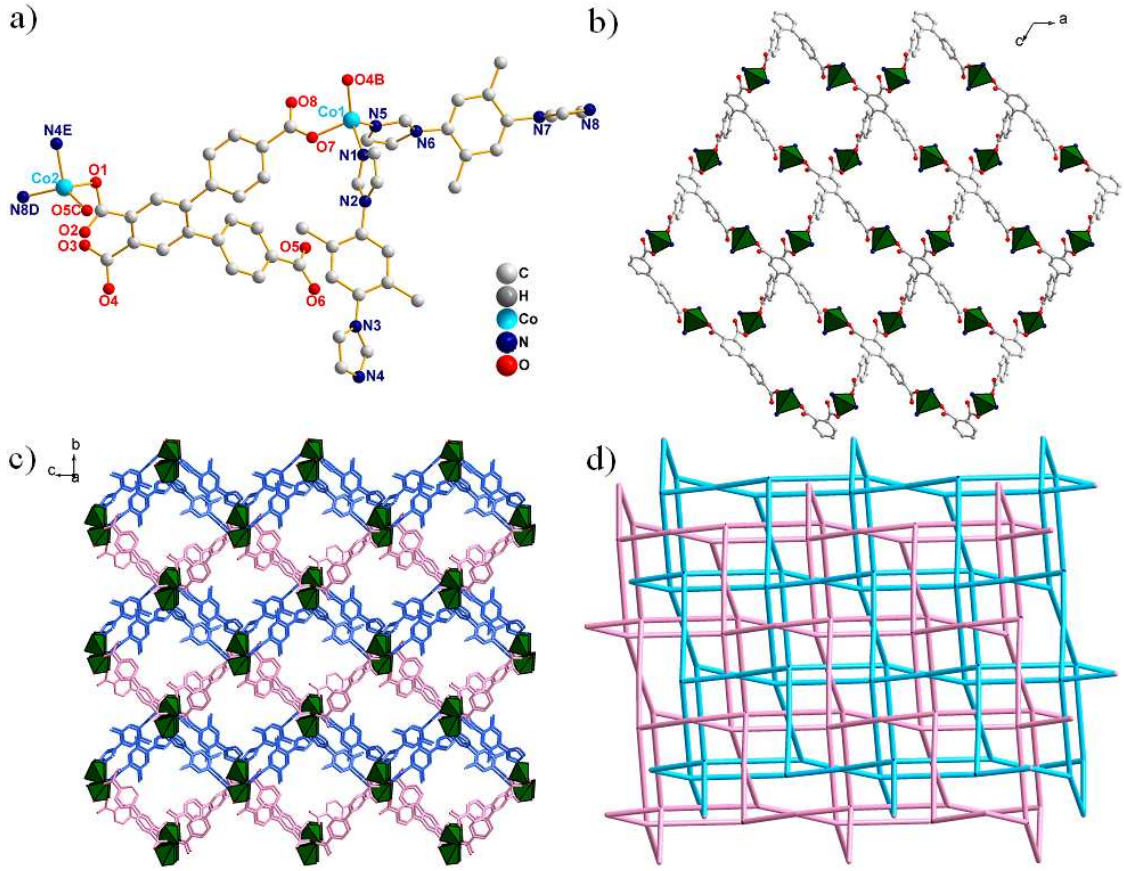

Figure 4. (a) Coordination environment of Co^{II} ions in **4** (Symmetry codes: B: 1+*x*, 0.5–*y*, 0.5+*z*; C: *x*, 0.5–*y*, –0.5+*z*; D: –1+*x*, –1+*y*, –1+*z*; E: *x*, –1+*y*, *z*.). (b) View of the 2D $[Co_2(DCP)]_n$ networks. (c) The 3D porous frameworks of **4**. (d) Schematic view of the 2-fold (4,4)-connected **bbf** network of **4**.

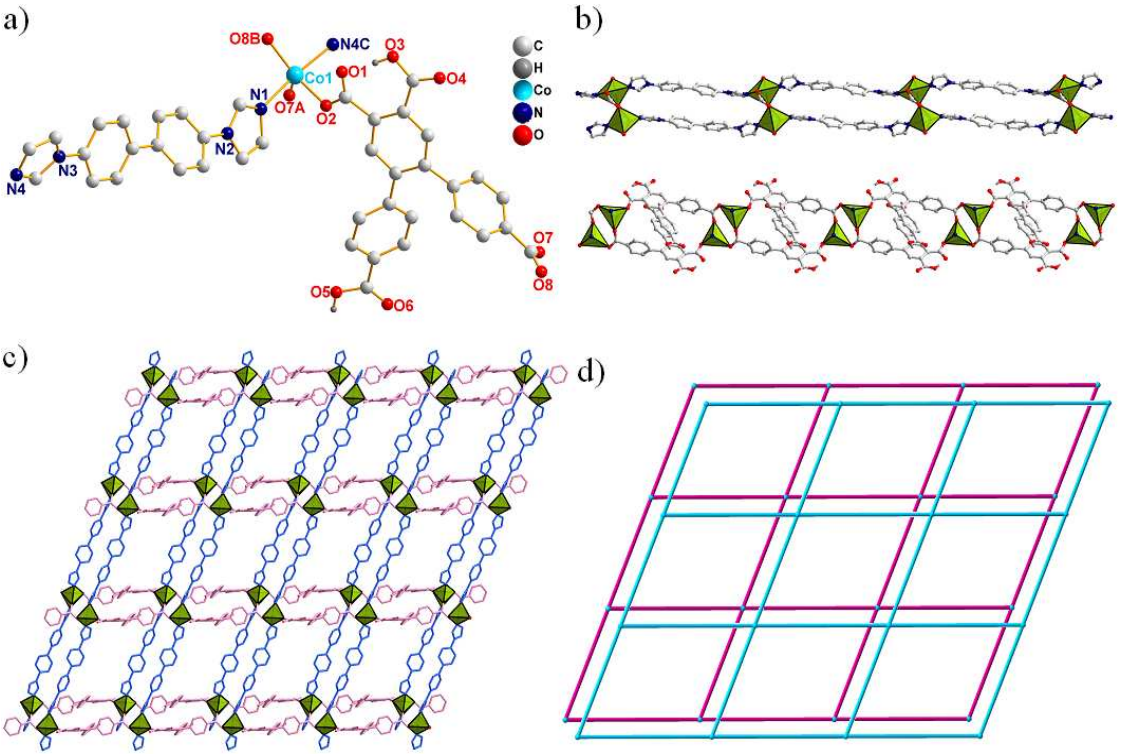

Figure 5. (a) Coordination environment of Co^{II} ions in **5** (Symmetry codes: A: –*x*, –*y*, 2–*z*; B: 1+*x*, *y*, –1+*z*; C: –1+*x*, –1+*y*, *z*.). (b) View of the 1D $[Co(H_2DCP)]_n$ chain and the 1D $[Co(4,4'\text{-bibp})]_n$ chain. (c) The 2D bilayer structure of **5**. (d) Schematic view of the 4-connected **sql** sheet of **5**.

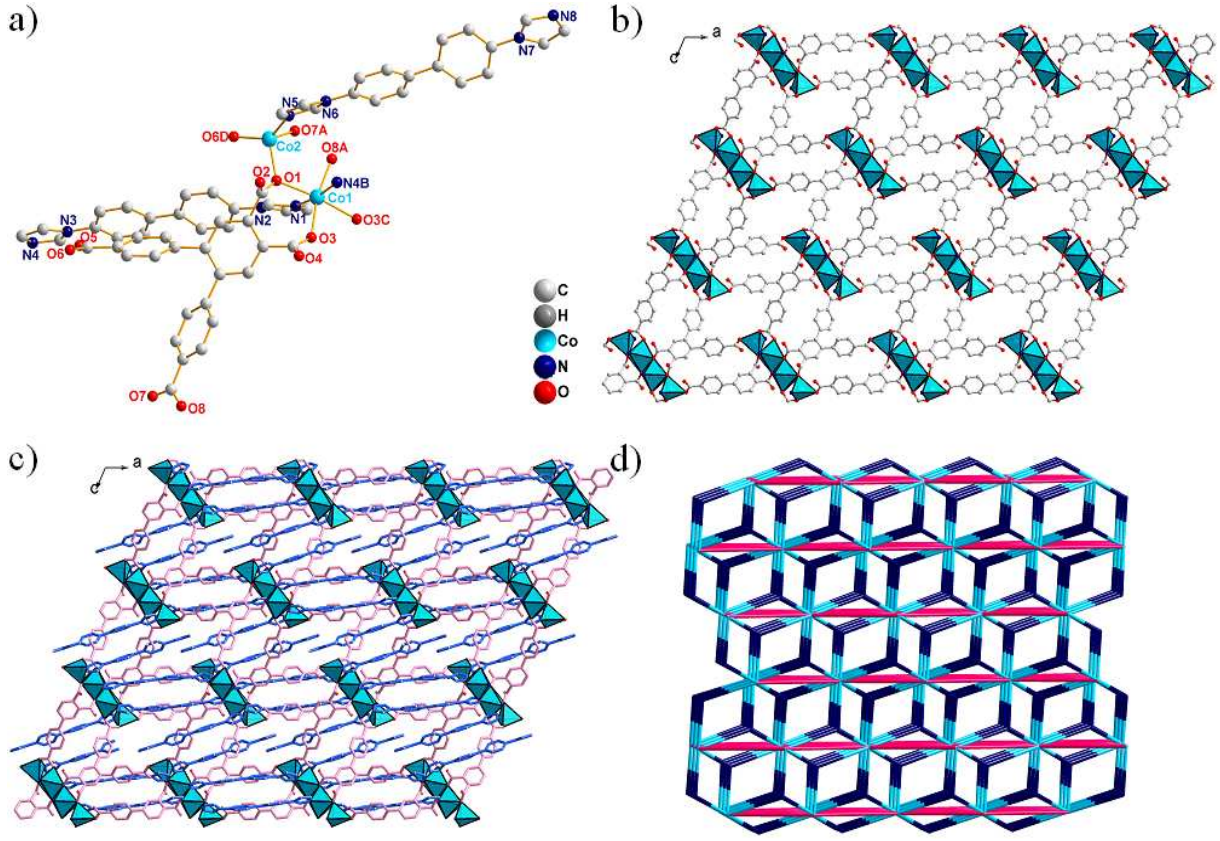

Figure 6. (a) Coordination environment of Co^{II} ions in **6** (Symmetry codes: A: *x*, 1–*y*, 0.5+*z*; B: –0.5+*x*, 0.5+*y*, *z*; C: 1–*x*, 1–*y*, 1–*z*; D: 1.5–*x*, 1.5–*y*, 1–*z*.). (b) View of the 3D $[Co_2(DCP)]_n$ frameworks. (c) The 3D structure frameworks of **6**. (d) Schematic view of the (3,8)-connected $(4^2.5)_2(4^4.5^{10}.6^8.7^4.8^2)$ net of **6** (green spheres: $\{Co_4\}$ SBUs; dakeblue spheres: DCP^{4-} ligands; red bonds: 4,4'-bibp ligands).

Table 3 The coordination modes of H_4DCP ligand and the roles of ancillary ligands in complexes **1**–**6**.

Complex	Coord. Modes	Ancillary Ligands/Role	Dihedral Angles (°) of H_4DCP	Structure and Topology
1	Mode I	1,4-bib/bridging	41.37(6)/52.05(2)/52.60(3)	1D+1D→1D cocrystal
2	Mode II	1,4-bidb/bridging	45.76(1)/53.59(4)/66.70(8)	2-fold 3D+3D→3D 4-connected 6^6-**dia** net
3	Mode III	1,3-bib/bridging	74.59(3)/54.56(0)/70.77(7)	3D (5,7)-connected $(3.4^4.5^4.6)(3^2.4^8.5^8.6^3)$ net
4	Mode IV	1,4-bidb/bridging	60.11(6)/56.98(7)/52.72(5)	2-fold 3D+3D→3D (4,4)-connected $(6^4.8^6)(6^6)_2$-**bbf** net
5	Mode V	4,4'-bibp/bridging	39.38(0)/75.39(5)/67.72(2)	2D 4-connected $(4^4.6^2)$-**sql** sheet
6	Mode VI	4,4'-bibp/cheating	64.95(3)/45.47(5)/53.66(0)	3D (3,8)-connected $(4^2.5)_2(4^4.5^{10}.6^8.7^4.8^2)$ net

Structure descriptions of $[Co_2(DCP)(4,4'\text{-bibp})_2]_n$ (6). With more NaOH being added to the reaction environment, H_4DCP is completely deprotonated and shows more complicated coordination mode, leaving a 3D framework containing $\{Co_4\}$ clusters. Complex **6** crystallizes in the monoclinic system with space group *P*-1. As shown in Fig. 6a, there are two Co^{II} ions, one completely deprotonated DCP^{4-} anion, and two 4,4'-bibp ligands in the asymmetric unit. It is noteworthy that the two independent Co^{II} ions hold different coordination geometries: Co(1) is hexa-coordinated with two N atoms from two individual 4,4'-bibp ligands and four O atoms from three DCP^{4-} anions. While Co(2) is tetra-coordinated, completed by three O atoms from three different DCP^{4-} ligands and One N atom from one the terminal 4,4'-bibp ligand. The Co–O and Co–N bond lengths are in the range of 1.976(2)–2.197(2) Å and 2.021(3)–2.118(3) Å, respectively.

In complex **6**, the DCP^{4-} anion shows $(\kappa^0\text{-}\kappa^2)\text{-}(\kappa^2\text{-}\kappa^0)\text{-}(\kappa^1\text{-}\kappa^1)\text{-}(\kappa^1\text{-}\kappa^0)\text{-}\mu_6$ coordination mode (Mode VI). The Co^{II} cations are bridged by $(\kappa^2\text{-}\kappa^0)\text{-}\mu_2$ and $(\kappa^1\text{-}\kappa^1)\text{-}\mu_2$ carboxyl groups, generating an unprecedented tetranuclear $\{Co_4\}$ cluster based SBUs with the Co···Co distances being 3.520 Å for Co1-Co2, 3.361 Å for Co1-$Co1^{\#1}$(Symmetry codes: #1: 1–*x*, 1–*y*, 1–*z*.), and 6.800 Å for Co2-$Co1^{\#1}$ (Fig. S6). Each $\{Co_4\}$ SBUs are connected with six DCP^{4-} anions, constructed a 3D (3,6)-connected networks (Fig. 6b). The networks are further solified by linkage of 4,4'-bibp ligands (Fig. 6c). Notably, only half of 4,4'-bibp ligands act as pillars to support the framework, meanwhile, the excess 4,4'-bibp ligands terminal coordinated with $\{Co_4\}$ SBUs to support the stability of the final structure with non-covalent interactions.

From the topological view, the $\{Co_4\}$ cluster based SBUs can be simplified as a 8-connected node, the DCP^{4-} anion as 3-connected node, the pillared 4,4'-bibp ligands are taken as linkers and the 3D structure can be classified as a novel (3,8)-connected architecture with the point symbol of $(4^2.5)_2(4^4.5^{10}.6^8.7^4.8^2)$ (Fig. 6d).

The Structural Comparison and Discussion. As shown in the Scheme 2 and Table 3, H_4DCP exhibits versatile coordination modes, with the deprotonated carboxyl groups coordinating one

or more metal ions. In complex **1**, the H_4DCP is partly deprotonated with $(\kappa^1\text{-}\kappa^0)\text{-}\mu_1$ coordination mode (Mode I), modified the 1D $[Ni(1,4\text{-bib})]_n$ chain by sharing the nickel ions. And the ionized carboxyl groups interact with another 1D $[Ni(1,4\text{-bib})(H_2O)_4]_n$ chain, act as both hydrogen bond acceptor and the charge balancing. It is belived the hrdrogen bonds as well as $\pi\cdots\pi$ interactions are critical in maintaining the overall cocrystal stability. When the 1,4-bib was changed to 1,4-bidb in complex **2**, the methyl steric effects make the final packing structure tend to form a diamond nets, with the partly deprotonated H_2DCP anion act as terminal group, occupied the porous channels to modify the networks. Complexes **3–6** are Co-based complexes and they were tuned by different bis(imidazole) linkers. The H_4DCP ligand in complex **3** are completely deprotonated and exhibit $(\kappa^1\text{-}\kappa^1)\text{-}(\kappa^2\text{-}\kappa^1)\text{-}(\kappa^1\text{-}\kappa^2)\text{-}(\kappa^1\text{-}\kappa^1)\text{-}\mu_8$ coordination mode (Mode III), with the four carboxylate groups show $(\kappa^1\text{-}\kappa^1)\text{-}\mu_2$, $(\kappa^1\text{-}\kappa^2)\text{-}\mu_2$ and $(\kappa^1\text{-}\kappa^2)\text{-}\mu_3$ coordination fashions, respecively. The two neighoubring Co^{II} ions are connected by $(\kappa^1\text{-}\kappa^2)\text{-}\mu_3$ and $(\kappa^1\text{-}\kappa^2)\text{-}\mu_2$ carboxylate groups, affording a $\{Co_2\}$ cluster by edge-sharing with the distance is 3.172 Å between Co1 and Co2. And the $\{Co_2\}$ clusters are further connected by the $(\kappa^1\text{-}\kappa^1)\text{-}\mu_2$ carboxylate groups, finally give an unusual 1D $[Co_4(COO)_8]_n$ chain. Then the 1D $[Co_4(COO)_8]_n$ chains linked with the DCP^{4-} and 1,3-bib ligands to yield a high-connected frameworks. As to complex **4**, all of carboxylate groups in DCP^{4-} exhibit simple κ^1 fashion (Mode IV), linked the four Co^{II} into a 2D $[Co_2(DCP)]_n$ networks, which further constructed the 3D networks with the help of bridging 1,4-bidb linkers. For complex **5**, the partly deprotonated H_2DCP^{2-} ligand used its $(\kappa^1\text{-}\kappa^1)\text{-}\mu_2$ carboxylate groups (Mode V) to link two Co^{II} ions, forming a $[Co_2(COO)_2]$ SBUs with the Co1$\cdots$Co2 separation is 3.702 Å. Then the H_2DCP^{2-} as well as the 4,4'-bibp ligands act as pillars to support a 2D networks. Compared with complex **5**, the coordination mode (Mode VI) of H_4DCP in complex **6** are more complicated when more NaOH was added. Four carboxylate groups in complex **6** adopt $(\kappa^0\text{-}\kappa^2)\text{-}\mu_2$, $(\kappa^1\text{-}\kappa^1)\text{-}\mu_2$ and simple κ^1 coordination fashions, respectively. The adjacent Co ions are connected by the $(\kappa^0\text{-}\kappa^2)\text{-}\mu_2$ and $(\kappa^1\text{-}\kappa^1)\text{-}\mu_2$ carboxylate groups, affording a $[Co_4(COO)_6]$ SBUs. The $[Co_4(COO)_6]$ SBUs linked with six DCP^{4-} ligands and four bridging 4,4'-bibp ligands, formed an unprecedented 3,8-connected frameworks.

To the best of our knowledge, all of the coordination modes have never been documented up to now, which also indicated the bis(imdizaole) ancillary linkers have great influences on the coordination modes of H_4DCP. Besides, the employment the bis(imidazole) bridging linkers in assemble of metal–polycarboxylates coordination polymers often leads to structural changes and affords unprecedented architectures since they can modulate their conformations and coordination modes to fine-tune themselves to satisfy the coordination preference of metal centers or metal cluster. The comparisons between those complexes revealed that not only internal factors, but also the external factors have great influences on the coordination modes of polycarboxylates and final packing structures.

Thermal Analyses. The experiments of thermogravimetric analysis (TGA) were performed on samples of complexes **1**-**6** under N_2 atmosphere with a heating rate of 10 °C min^{-1}, shown in Fig. S6. For complex **1**, the first weight loss in the temperature range of 80-130°C is consistent with the removal of the coordinated and lattice water molecules (obsd 13.5 %, calcd 14.2 %). And then the packing structure starts to collapse since the hydrogen bonds were broken. For complex **2**, an initial weight loss of 2.3 % corresponds to the loss of coordinated water molecules (calcd: 1.9 %). The second weight loss corresponds to the loss of the organic ligands. For complex **3**, the framework is stable until 380°C, and then it starts to lose its ligands as a result of thermal decomposition with the final remaining weight is ca. 23.4 % (calcd. for Co_2O_3 22.7 %). The TGA curve of complex **4** displays the first loss of 4.2 % in the temperature range of 90-140°C corresponding to the loss of lattice water molecules. And then the neutral framework collapses with the temperature increasing. Complex **5** began to release the organic ligands from 250°C with the final residual weight being ca. 12.3 % (calcd. for Co_2O_3 11.1 %). For complex **6**, the overall structure is stable until 370°C, and then the decomposition of organic ligands began, finally giving a residual weight of ca. 16.7 % (calcd. for Co_2O_3 15.2 %).

Magnetic Properties. The variable-temperature magnetic susceptibility of **3** and **6** were performed in the temperature range of 1.8-300 K under a field of 1000 Oe because the $[Co_4(COO)_8]_n$ chain in complex **3** and the $[Co_4(COO)_6]$ SBUs in complex **6** maybe own excellent magnetic properties. The temperature dependence of $\chi_M T$, χ_M and χ_M^{-1} versus T are displayed in Fig. 7 and 8.

The $\chi_M T$-T plot in Fig.7 proved that complex **3** holds weak ferromagnetic character. The $\chi_M T$ value at room temperature is 4.48 cm^3 K mol^{-1}, and decreases to the lowest value of 2.94 cm^3 K mol^{-1} at 10 K with the temperature steadily declining. Then the plot increases to 3.68 cm^3 K mol^{-1} at 1.8 K indicating a weak ferromagnetic interaction between neighbouring Co ions. [17]

For complex **6**, the $\chi_M T$ value is 9.75 cm^3 K mol^{-1} at room temperature, and then decrease evenly as temperature reduces, finally reached 2.21 cm^3 K mol^{-1} at about 1.8 K (Fig. 8). The temperature dependence χ_M^{-1} obey the Curie-Weiss law $\chi_M = C/(T-\theta)$ with C= 10.50 cm^3 K mol^{-1}, θ= –19.33 K. The negative θ value demonstrate the existence of antiferromagnetic interactions between adjacent Co centers. [18]

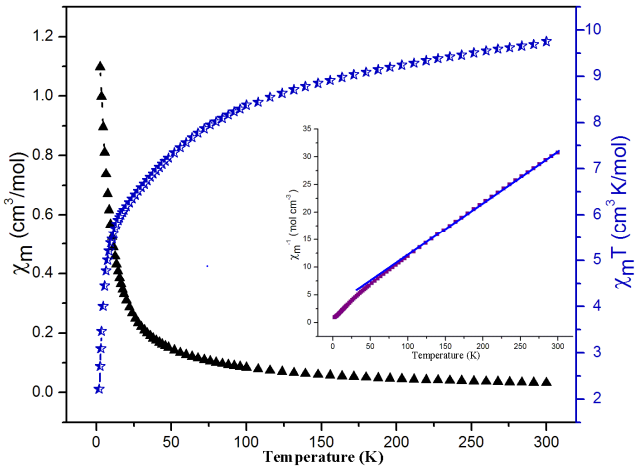

Figure 7. The temperature dependence of magnetic susceptibility of **3** under a static field of 1000 Oe.

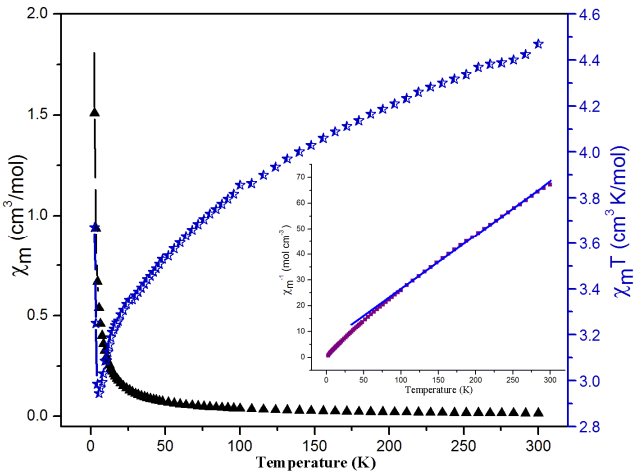

Figure 8. The temperature dependence of magnetic susceptibility of **6** under a static field of 1000 Oe.

Conclusions

In summary, six CPs were synthesized based on 4,5-di(4'-carboxylphenyl)phthalic acid (H_4DCP) and four different bis(imidazole) bridging linkers (1,3-bib, 1,4-bib, 1,4-bidb, and 4,4'-bibp) under hydrothermal conditions, with the final packing structures exhibit a systematic variation of architectures from 1D chains based cocrystal, 2D networks, to 3D frameworks. These results reveal that not only the nature of the bridging bis(imidazole) linkers (length, functional groups or substituent position) but also the reaction conditions (pH, metal ion, metal-ligand ratio) have great effect on the H_4DCP coordination modes and the final packing structures. Moreover, magnetic studies indicate complex **3** exhibit very weak ferromagnetic character and **6** show antiferromagnetic property.

Acknowledgements

The work was supported by financial support from the Natural Science Foundation of China (Grant Nos. 21101097, 91022034 and 51172127), the Excellent Youth Foundation of Shandong Scientific Committee (Grant JQ201015), and Qilu Normal University is acknowledged.

Notes

The authors declare no competing financial interest.

References

1. (a) M. Zhang, W. Lu, J. R. Li, M. Bosch, Y. P. Chen, T. F. Liu, Y. Liu and H. C. Zhou, *Inong. Chem. Front.*, 2014, **1**, 159; (b) J. Duan, M. Higuchi, R. Krishna, T. Kiyonaga, Y. Tsutsumi, Y. Sato, Y. Kubota, M. Takata and S. Kitagawa, *Chem. Sci.*, 2014, **5**, 660; (c) B. L. Chen, N. W. Ockwig, A. R. Millward, D. S. Contreras and O. M. Yaghi, *Angew. Chem. Int. Ed.*, 2005, **44**, 4745; (d) J. Duan, Z. Yang, J. Bai, B. Zheng, Y. Li and S. Li, *Chem. Commun*., 2012, **48**, 3058; (e) P. V. Dau and S. M. Cohen, *Chem. Commun.*, 2013, **49**, 6128.
2. (a) G. Férey and C. Serre, *Chem. Soc. Rev*., 2009, **38**, 1380; (b) H. Fei, J. F. Cahill, K. A. Prather and S. M. Cohen, *Inorg. Chem.*, 2013, **52**, 4011; (c) M. Kim, J. F. Cahill, H. Fei, K. A. Prather and S. M. Cohen, *J. Am. Chem. Soc*., 2012, **134**, 18082; (d) Y. Cui, Y. Yue, G. Qian and B. L. Chen, *Chem. Rev.*, 2012, **112**, 1126.
3. (a) D. Sun, S. Yuan, H. Wang, H. F. Lu, S. Y. Feng and D. F. Sun, *Chem. Commun*., 2013, **49**, 6152; (b) X. T. Zhang, L. M. Fan, X. Zhao, D. Sun, D. C. Li and J. M. Dou, *CrystEngComm*, 2012, **14**, 2053; (c) X. Zhang, L. Fan, W. Zhang, Y. Ding, W. Fan and X. Zhao, *Dalton. Trans*., 2013, **42**, 16562; (d) J. B. Lin, W. Xue, B. Y. Wang, J. Tao, W. X. Zhang, J. P. Zhang and X. M. Chen, *Inorg. Chem*., 2012, **51**, 9423; (e) K. Wang, S. Zeng, H. Wang, J. Dou and J. Jiang, *Inong. Chem. Front.*, 2014, **1**, 167.
4. (a) F. Cao, S. Wang, D. Li, S. Zeng, M. Niu, Y. Song and J. Dou *Inorg. Chem.*, 2013, **52**, 10747; (b) X. T. Zhang, D. Sun, B. Li, L. M. Fan, B. Li and P. H. Wei, *Cryst. Growth Des.*, 2012, **12**, 3845; (c) J. Gao, Y. Gao, Y. Wang, C. Du and Z. Li, *Chem. Commun*., 2013, **49**, 6897; (d) J. Y. Zou, W. Shi, H. L. Gao, J. Z. Cui and P. Cheng, *Inong. Chem. Front.*, 2014, **1**, 242.
5. (a) S. Chen, R. Shang, K. L. Hu, Z. M. Wang and S. Gao, *Inong. Chem. Front.*, 2014, **1**, 83; (b) Y. Wang, H. X. Lin, L. Chen, S. Y. Ding, Z. C. Lei, D. Y. Liu, X. Y. Cao, H. J. Liang, Y. B. Jiang and Z. Q. Tian, *Chem. Soc. Rev*., 2014, **43**, 399; (c) H. Zhou, G. X. Liu, X. F. Wang and Y. Wang, *CrystEngComm.*, 2013, **15**, 1377; (d) S. Y. Song, X. Z. Song, S. N. Zhao, C. Qin, S. Q. Su, M. Zhu, Z. M. Hao and H. J. Zhang, *Dalton. Trans*., 2012, **41**, 10412.
6. (a) L. Li, J. Ma, C. Song, T. Chen, Z. Sun, S. Wang, J. Luo and M. Hong, *Inorg. Chem.*, 2012, **51**, 2438; (b) C. C. Ji, J. Li, Y. Z. Li, Z. J. Guo and H. G. Zheng, *CrystEngComm.,* 2011, **13**, 459; (c) D. Sun, L. L. Han, S. Yuan, Y. K. Deng, M. Z. Xu and D. F. Sun, *Cryst. Growth Des.*, 2013, **13**, 377; (d) X. Zhang, L. Fan, Z. Sun, W. Zhang, W. Fan, L. Sun and X. Zhao, *CrystEngComm*, 2013, **15**, 4910.
7. (a) X. H. Chang, J. H. Qin, M. L. Han, L. F. Ma and L. Y. Han, *CrystEngComm*, 2014, **16**, 870; (b) N. Zhang, Y. Tai, M. Liu, P. Ma, J. Zhao and J. Niu, *Dalton Trans.,* 2014, **43**, 5182; (c) W. Meng, Z. Xu, J. Ding, D. Wu, X. Han, H. Hou and Y. Fan, *Cryst. Growth Des.*, 2014, **14**, 730; (d) L. Fan, X. Zhang, D. Li, D. Sun, W. Zhang and J. Dou, *CrystEngComm*, 2013, **15**, 349.
8. (a) J. J. Wang, T. T. Wang, L. Tang, X. Y. Hou, M. L. Zhang, L. J. Gao, F. Fu and Y. X. Ren, *Z. Anorg. Allg. Chem.*, 2014, **640**, 483; (b) Y. B. Wang, Y. L. Lei, S. H. Chi and Y. J. Luo, *Dalton Trans.,* 2013, **42**, 1862; (c) Q. Yu, Q. Zhang, H. Bian, H. Liang, B. Zhao, S. Yan and D. Liao, *Cryst. Growth Des.*, 2008, **8**, 1140; (d) X. Zhang, L. Fan, Z. Sun, W. Zhang, D. Li, J. Dou and L. Han, *Cryst. Growth Des.*, 2013, **13**, 792.
9. (a) G. L. Liu and H. Liu, *CrystEngComm*, 2013, **15**, 6870; (b) C. Zhan, C. Zou, G. Q. Kong and C. D. Wu, *Cryst. Growth Des.*, 2013, **13**, 1429; (c) J. J. Wang, T. T. Wang, L. Tang, X. Y. Hou, L. J. Gao, F. Fu and M. L. Zhang, *J. Coord. Chem.*, 2013, **66**, 3979; (d) L. Fan, X. Zhang, Z. Sun, W. Zhang, Y. Ding, W. Fan, L. Sun, X. Zhao and H. Lei, *Cryst. Growth Des.*, 2013, **13**, 2462.
10. (a) Q. L, Zhang, G. W. Feng, Y. Q. Zhang and B. X. Zhu, *RSC Advances*, 2014, **4**, 11384; (b) B. Guo, L. Li, Y. Wang, Y. Zhu and G. Li, *CrystEngComm*, 2013, **42**, 14268; (c) M. L. Han, S. C. Wang and D. F. Feng, *Cryst. Res. Technol.*, 2014, **49**, 276; (d) Q. L. Zhang, P. Hu, Y. Zhao, G. W. Feng, Y. Q. Zhang, B. X. Zhu and Z. Tao, *J. Solid State Chem.*, 2014, **210**, 178.
11. (a) F. Guo, B. Zhu, M. Liu, X. Zhang, J. Zhang and J. Zhao, *CrystEngComm*, 2013, **15**, 6191; (b) L. Fan, X. Zhang, W. Zhang, Y. Ding, W. Fan, L. Sun, Y. Pang and X. Zhao, *Dalton Trans.,* 2014, **43**, 6701; (c) X. Zhang, L. Fan, W. Zhang, W. Fan, L. Sun and X. Zhao, *CrystEngComm*, 2014, **16**, 3203; (d) B. Liu, L. Wei, N. N. Li, W. P. Wu, H. Miao, Y. Y. Wang and Q. Z. Shi, *Cryst. Growth Des*., 2014, **14**, 1110.
12. (a) M. L. Han, X. H. Chang, X. Feng, L. F. Ma and L. Y. Wang, *CrystEngComm*, 2014, **16**, 1687; (b) C. Q. Wang, Y. Zhang, X. Z. Sun and H. J. Yan, *CrystEngComm*, 2014, **16**, 2959; (c) X. L. Wang, Y. Qu, G. C. Liu, J. Luan, H. Y. Lin and X. M. Kan, *Inorg. Chem. Acta*, 2014, **412**, 104; (d) K. K. Bisht, Y. Rachuri, B. Parmar and E. Suresh, *J. Solid State Chem.*, 2014, **213**, 43.
13. (a) L. L. Liu, C. X. Yu, Y. Zhou, J. Sun, P. P. Meng, D. Liu and R. J. Sa, *Inorg. Chem. Commun*, 2014, **40**, 194; (b) X. T. Zhang, L. M. Fan, Z. Sun, W. Zhang, D. C. Li, J. M. Dou and L. Han, *Cryst. Growth Des*., 2013, **13**, 792; (c) X. T. Zhang, L. M. Fan, W. Zhang,

Y. S. Ding, W. L. Fan, L. M. Sun, X. Zhao and H. Lei, *Cryst. Growth Des*., 2013, **13**, 2462; (d) L. Fan, X. Zhang, W. Zhang, Y. Ding, L. Sun, W. Fan and X. Zhao, *CrystEngComm*, 2014, **16**, 2144.

14. (a) G. M. Sheldrick, *SHELXTL*, version 5.1; Bruker Analytical X-ray Instruments Inc.: Madison, WI, 1998. (b) G. M. Sheldrick, *SHELX-97*, PC Version; University of Gottingen: Gottingen, Germany, 1997.
15. (a) V. A. Blatov, A. P. Shevchenko and V. N. Serezhkin, *J. Appl. Crystallogr.*, 2000, **33**, 1193; (b) The network topology was evaluated by the program "TOPOS-4.0", see: http://www.topos.ssu.samara.ru. (c) V. A. Blatov, M. O'Keeffe and D. M. Proserpio, *CrystEngComm*, 2010, **12**, 44.
16. (a) A. L. Spek, *J. Appl. Crystallogr.*, 2003, **36**, 7; (b) A. L. Spek, *PLATON, A Multipurpose Crystallographic Tool*, Utrecht University, Utrecht, The Netherlands, 2002.
17. (a) P. Lama, J. Mrozinski and P. K. Bharadwaj, *Cryst. Growth Des.*, 2012, **12**, 3158; (b) M. Ahmad, M. K. Sharma, R. Das, P. Poddar and P. K. Bharadwaj, *Cryst. Growth Des.*, 2012, **12**, 1571; (c) A. Mukherjee, R. Raghunathan, M.K. Saha, M. Nethaji, S. Ramasesha and A.R. Chakravarty, *Chem. Eur. J.*, 2005, **11**, 3087;
18. (a) L. Y. Pang, P. Liu, C. P. Zhang, X. Chen, B. Chen, Y. Y. Wang and Q. Z. Shi, *Inong. Chem. Acta*, 2013, **403**, 43; (b) O. Kahn, *Molecular Magnetism*, Wiley-VCH, New York, 1993.

CrystEngComm
For Table of Contents Use Only

Table of Contents Graphic and Synopsis

Syntheses, Structures, and Magenetic Properties of Six Coordination Polymers Based on 4,5-Di(4'-carboxylphenyl)phthalic Acid and Different Bis(imidazole) Bridging Linkers

Liming Fan, Yan Gao, Guangzeng Liu, Weiliu Fan, Weiku**o Song, Liming Sun, Xian Zhao, Xiutang Zhang**

Hydrothermal reactions based on 4,5-di(4'-carboxylphenyl)phthalic acid (H_4DCP) and transitional metal cations in the presence of four different bis(imidazole) bridging linkers (1,3-bib, 1,4-bib, 1,4-bidb, 4,4'-bibp) afford six new coordination polymers. Compounds **1**-**6** displayed diverse structural features from 1D chain, 2D networks to 3D frameworks.